APL MATERIALS **5**, 056101 (2017)

Ultrafast relaxation of hot phonons in graphene-hBN heterostructures

Dheeraj Golla, Alexandra Brasington, Brian J. LeRoy, and Arvinder Sandhu[a]
Department of Physics, University of Arizona, Tucson, Arizona 85721, USA

(Received 20 January 2017; accepted 17 April 2017; published online 8 May 2017)

Fast carrier cooling is important for high power graphene based devices. Strongly coupled optical phonons play a major role in the relaxation of photoexcited carriers in graphene. Heterostructures of graphene and hexagonal boron nitride (hBN) have shown exceptional mobility and high saturation current, which makes them ideal for applications, but the effect of the hBN substrate on carrier cooling mechanisms is not understood. We track the cooling of hot photo-excited carriers in graphene-hBN heterostructures using ultrafast pump-probe spectroscopy. We find that the carriers cool down four times faster in the case of graphene on hBN than on a silicon oxide substrate thus overcoming the hot phonon bottleneck that plagues cooling in graphene devices. [http://dx.doi.org/10.1063/1.4982738]

Graphene heterostructures have garnered a lot of interest in the last decade.[1] Recently developed fabrication techniques have made it possible to engineer devices with better transport, optical, and thermal properties.[2,3] Hexagonal boron nitride (hBN) is a layered material with a hexagonal lattice similar to graphene with a lattice constant that is about 1.8% larger.[3] It is an insulator with a wide band gap and high dielectric constant making it a good candidate as a substrate for graphene devices. Heterostructures of graphene and hBN show much higher mobility compared to those using SiO_2 as a substrate.[2–4] This improvement is a result of the hBN substrate being free of charged impurities and displacing the graphene away from the impurities in the SiO_2 substrate.[4]

As electronic devices continue to scale down in size and push power capabilities, heat management has become a critical issue. Relaxation dynamics of photoexcited (PE) carriers has been studied extensively by many groups using a variety of techniques such as photocurrent measurement, time resolved Raman spectroscopy, transport measurements, ultrafast pump-probe spectroscopy,[5–7] etc. Upon photoexcitation (with an ultrafast pulse, for example), electrons and holes are excited into a highly non-thermal system. The carriers exchange energy among themselves through Coulombic interactions and thermalize into a hot (~1000's K) Fermi-Dirac population within tens of femtoseconds.[8] This hot thermal population cools further through the emission of optical phonons near the Γ point of the phonon dispersion. When the temperatures of the carriers and optical phonon bath equalize, this cooling channel slows down and this is termed as the Hot Phonon (HP) bottleneck.[5,9–13] Cooling through direct acoustic phonon emission is not viable because of a vanishingly small phase space for such a scattering process.[14] The hot optical phonons cool down through anharmonic decay to acoustic phonons which are subsequently absorbed into the substrate. Direct cooling of the charge carriers is also predicted to occur through coupling with the surface phonons of the underlying polar substrate.[12,15–17] Theoretical predictions and experiments place the hot optical phonon lifetime in graphene, graphite, and carbon nanotubes in the 1–5 ps range.[5,9,18–21] The buildup of optical phonons is detrimental to device performance and the HP bottleneck has been invoked to explain current saturation and negative differential conductance in graphene and carbon nanotubes.[10,11,22] The HP bottleneck also affects the photoresponse[23] of optoelectronic devices. It is important to explore cooling channels that can efficiently de-energize the optical phonons and remove the HP bottleneck. In

[a]asandhu@email.arizona.edu

that regard, graphene heterostructures incorporating an appropriate substrate, such as hBN, could offer additional mechanisms for accelerating the cooling process. It has been recently reported that the active cooling efficiency due to the Peltier effect in graphene-hBN devices is more than twice as much as the highest reported room temperature efficiencies.[24] A comparative study of relaxation dynamics for graphene on hBN and SiO_2 is missing from the literature. In this letter, we study the relaxation of carriers in graphene-hBN heterostructure devices. Our findings indicate that the substrate interface plays a major role in the carrier cooling process and carriers in graphene devices fabricated on hBN substrates relax significantly faster than those on SiO_2 substrates thus providing relief of the HP bottleneck and enabling better device performance.

Hexagonal boron nitride flakes were exfoliated and deposited on silicon chips that have a 285 nm thermally grown oxide layer. Pristine graphene was grown on copper foil using a low pressure chemical vapor deposition (CVD) method as described in the work by Xuesong Li *et al.*[25] PMMA was spin coated onto the copper foil before floating it on a mixture of hydrogen peroxide, hydrochloric acid, and de-ionized water to etch away the copper. The remaining graphene/PMMA film was transferred to clean de-ionized water. The Si/SiO_2 chip with exfoliated hBN was used to gently pick up the floating graphene/PMMA film and then dried. The chip was then placed in acetone to dissolve the PMMA layer. The samples were then subsequently annealed in an atmosphere of argon and hydrogen at 350 °C for 3 h to get rid of residues and impurities and ensure better adhesion to the substrate. An optical image of one of the samples is shown in Figure 1. The spot marked 1 has graphene on hBN (g-hBN), whereas spot 2 has graphene on SiO_2 (g-SiO_2). The Raman spectra of g-SiO_2 and g-hBN are shown in Figure 1(b). The absence of a D peak means that both the g-SiO_2 and g-hBN are defect free. We infer from the G and 2D peak positions that g-SiO_2 and g-hBN are p-doped by about 3.5×10^{12} cm^{-2} and 1×10^{12} cm^{-2}, respectively.[26,27] The maximum energy of the doped carriers is well below the 1.58 eV probing photon energy.

For the pump-probe study we used amplified 780 nm pulses from a Ti-sapphire laser amplifier for both pump and probe. The spot sizes (FWHM) of the pump and probe beams were measured using the knife edge technique to be 154 μm and 23 μm, respectively. The FWHM as measured using the FROG technique was 45 fs. The experiment was conducted with a range of pump pulse energies, all of which were below the damage threshold of graphene under irradiation with ultrafast pulses.[28] The pump was chopped using an optical chopper and the probe reflectivity of the sample was measured using lock-in detection. The polarizations of the pump and probe were crossed for better rejection of the pump scatter.

The relaxation of PE carriers is captured by the differential reflectivity, $\frac{\Delta R(t)}{R_0}$, of the sample. The differential reflectivity shows the opposite trend as the electronic temperature in graphene, which means that a decrease in $\frac{\Delta R(t)}{R_0}$ corresponds to an increase in the electronic temperature. Figure 2 shows $\frac{\Delta R(t)}{R_0}$ as a function of the pump-probe time delay for three different g-hBN structures along with curves for g-SiO_2 for comparison. The pump pulse energy is 60 $\mu J/cm^2$. The baseline at large positive pump probe delay is non-zero because of the underlying contribution from silicon base of our

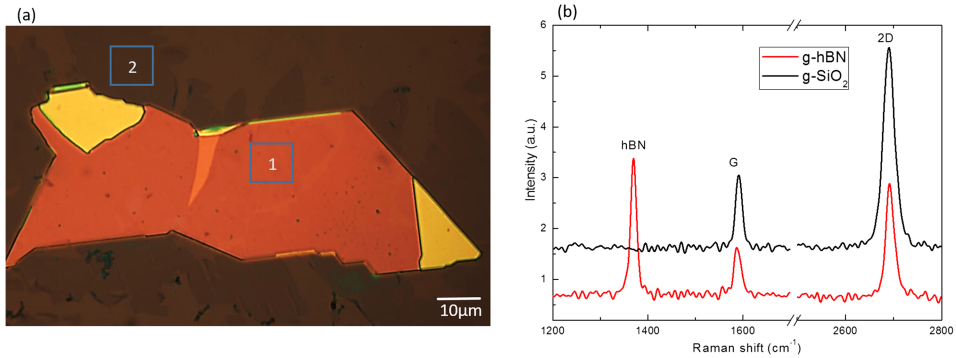

FIG. 1. (a) Optical image of sample 1. The mean thickness of the hBN flake shown here is 118 nm as measured using AFM. Spot marked 1 is g-hBN and spot marked 2 is g-SiO_2. (b) Raman spectra of the graphene on hBN (red) and on SiO_2 (black). The curves are vertically offset for clarity.

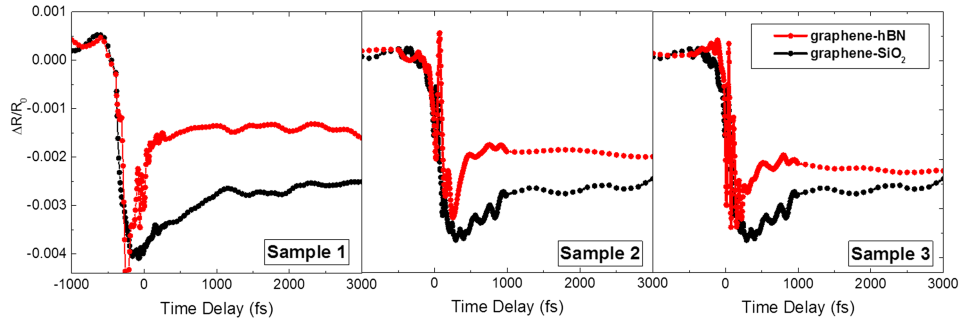

FIG. 2. Experimental differential reflectivity curves for different samples of g-hBN pumped using 60 μJ/cm^2 per pulse. The reflectivity of g-SiO_2 is shown for comparison (red: g-hBN and black: g- SiO_2).

samples. This baseline is constant over 100 ps which is a far greater time scale than those discussed in this letter. We have independently verified that this baseline does not contribute to the lifetimes extracted from our experiment (Section S2 in the supplementary material). It is immediately evident from Figure 2 that the relaxation dynamics of g-hBN are faster than that of g-SiO_2.

In order to quantify the time scales observed in the experiment, we modeled the temperature dynamics of the heterostructure using a two-temperature model.[29,30] The lateral transport of heat is negligible because the diffusion time scale is of the order of 90 μs (Section S1 in the supplementary material),

$$\frac{dT_{el}}{dt} = \frac{I(t) - \Gamma\left(T_{el}, T_{op}\right)}{c_{el}(T)}, \tag{1}$$

$$\frac{dT_{op}}{dt} = \frac{\Gamma\left(T_{el}, T_{op}\right)}{c_{op}(T)} - \frac{T_{op} - T_0}{\tau_{op}}, \tag{2}$$

where T_{el} and T_{op} denote the electronic and optical phonon temperatures of graphene, respectively. The coupling between T_{el} and T_{op} is given by the function $\Gamma(T_{el},T_{op})$. T_0 is the ambient room temperature; c_{op} and c_{el} denote the phononic and electronic heat capacity of graphene; $I(t)$ is the time profile of the pump pulse which is assumed to be Gaussian with a FWHM of 45 fs. The thermal relaxation time scale is τ_{op} which denotes the optical phonon lifetime in graphene. We numerically solve the system of differential equations given above for the electronic temperature, which determines the optical conductivity (σ) of graphene as a function of time. We use the optical conductivity calculated in the previous step to determine the total reflectance of the heterostructure using the transfer matrix method. We fit the experimental transient reflectivity curves using the two-temperature model to estimate the optical phonon relaxation lifetime τ_{op}. Refer to the supplementary material (Section S3) for a detailed explanation of the model. The results of the fitting process are shown in Figure 3. Figure 3(a) shows the relaxation for g-hBN pumped with pulse fluences of 80 μJ/cm^2 (orange), 60 μJ/cm^2 (green), and 50 μJ/cm^2 (blue) for which we extract optical phonon lifetimes of 375 fs, 250 fs, and 200 fs (±25 fs). Figure 3(b) shows the corresponding fits for g-SiO_2 and the corresponding lifetimes are 1500 fs, 1200 fs, and 800 fs (±50 fs). The evolution of the electron temperature and the time scale for electrons and phonons to equilibrate is governed by the interplay between the anharmonic decay time scale (τ_{op}), which represents coupling to the acoustic phonons and the substrate, and the electron-phonon coupling constant (β) as defined in the supplementary material. The fast decay of optical phonons in the case of g-hBN has an immediate cooling effect on the electronic temperature. As seen from the temperature profiles in the insets of Figure 3, for g-SiO_2, T_{el} and T_{op} equilibrate around 1200 K, whereas for g-hBN they cool down to 600 K before equilibrating. The phonon relaxation lifetimes in g-hBN are lower than those measured for g-SiO_2 by about a factor of four for all fluences indicating that additional cooling channels for graphene's optical phonons are available when hBN is used as the substrate. The range of values of τ_{op} for g-SiO_2 (0.8–1.5 ps) agrees well with previous measurements of the phonon lifetime in SiO_2 supported graphene.[13,21] At higher fluences (i.e., high initial carrier densities), multibody effects like carrier screening, plasmonic

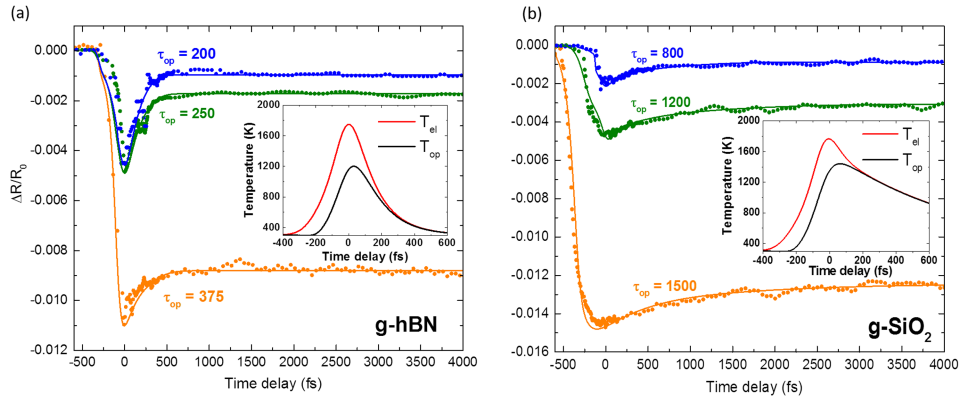

FIG. 3. (a) Differential reflectivity curves for graphene-hBN with different pump fluences: 80 μJ/cm^2 (orange), 60 μJ/cm^2 (green), and 50 (blue) μJ/cm^2. (b) Differential reflectivity curves for graphene-SiO_2 for the same fluences. Inset: Electronic (red) and phonon (black) temperature profiles for the case with the lowest fluence.

modes, and plasmon-phonon interactions might come into play.[31] While these multibody effects are not captured by the simple two temperature model, it still allows us to phenomenologically deduce the optical phonon relaxation lifetime. At low fluence where these multibody effects are relatively small, we can estimate the interfacial thermal conductance of the graphene–hBN interface from the optical phonon lifetimes using the lumped heat capacity model. The phonon lifetime is related to the interfacial conductance by the equation

$$G_k = \frac{c_{eff}}{\tau_{op}}, \tag{3}$$

where

$$\frac{1}{c_{eff}} = \frac{1}{c_{hBN}} + \frac{1}{c_{op} + c_{el}}. \tag{4}$$

The heat capacity c_{eff} is the effective heat capacity per unit area of the composite graphene-hBN system.[32] The heat capacity and conductance of hBN can be ignored because the limiting term in the vertical heat transport dynamics of the heterostructure is the interfacial thermal conductance between graphene and the substrate. We estimate the interfacial conductance for g-hBN to be 16.25 MW/m^2 K using the room temperature value for c_{eff} and the value of τ_{op} extracted from the 50 μJ/cm^2 fluence data. The corresponding value for the graphene-SiO_2 interface is 3.75 MW/m^2 K. Ideally, to estimate the room temperature thermal conductance, one would have to conduct the pump-probe experiment at extremely low pump fluence to ensure that the temperature change is minimal. Since we observe that optical phonon lifetime decreases with decreasing fluence, the measured phonon lifetime for such an experiment would be shorter. Accordingly, the room temperature interface thermal conductance would be higher than our estimate. Regardless, our estimates facilitate comparison between the relative thermal conductivities of g-hBN and g-SiO_2 interfaces under identical conditions, which is the main focus of our study. The value of G_k for g-hBN measured here is still higher than that reported in the work by Chen *et al.*[33] by more than a factor of two. The sample used in their experiment underwent electron beam lithography and oxygen plasma etching which might have possibly affected the interface quality and suppressed the interfacial conductance. As far as we know, there are no previous measurements of the relaxation of carriers in graphene on hBN. For the purpose of comparison, we can calculate the equivalent relaxation times from the alternate methods for measurements and predictions of the interfacial thermal conductivity of the graphene–hBN interface. The results are listed in Table I.

The interaction between the carriers in graphene and the surface plasmon polaritons (SPP) of the polar substrate has been proposed as a possible cooling mechanism for overcoming the HP bottleneck in graphene.[15–17,34] It has been established that graphene on hBN substrates has lower charge doping level than graphene on SiO_2[3] which is also the case in our samples as evidenced by the slightly upshifted (~10 cm^{-1}) and narrower G peak[27] for g-SiO_2. If SPP interactions were

TABLE I. Interfacial thermal conductance and thermal time constants for graphene on hBN.

Study	G_k(MW/m^2 K)	Thermal time constant (fs)	Notes
Mao *et al.*[35]	187	17	Room temperature, theoretical
Pak *et al.*[36]	4	800	Room temperature, theoretical
Chen *et al.*[33]	7.41	435	Room temperature, experimental
Zhang *et al.*[37]	3	1076	200–700 K, theoretical
Ting Li *et al.*[38]	1-10	300–3000	200–600, theoretical

the dominant cooling mechanism, the doping of graphene due to SiO_2 will shield this interaction and reduce the efficacy of this channel consequently increasing the relaxation time for phonons in g-SiO_2. The interaction between graphene and the substrate also depends on many factors like topographic conformity, Coulombic interactions, and adhesion energy. The g-hBN interface can be more transparent to heat carrying phonons because of the similar masses of carbon, boron, and nitrogen.[35] The curvature of the graphene sheet is an additional contributor to the interface thermal resistance in g-SiO_2.[36] Annealing contributes to the graphene sheet conforming to the substrate and hBN being atomically flat means the graphene sheet in g-hBN has lower cumulative curvature than the graphene sheet in g-SiO_2 effectively decreasing interfacial resistance in g-hBN.

In conclusion, we have used differential reflectance spectroscopy to study the carrier dynamics of graphene-hBN heterostructures. We extract the optical phonon lifetime and interface thermal conductance using a two-temperature model. The thermal relaxation rates of graphene-hBN are significantly faster than those of graphene-SiO_2 thus mitigating the hot phonon bottleneck. We conclude that hBN substrates will enhance the thermal performance of high power graphene devices.

Note added in proof. Faster relaxation of carriers in graphene-hBN heterostructures has also recently been observed through photoconductivity measurements and attributed to hyperbolic phonon coupling.[39]

See supplementary material for the following sections: S1—Lateral heat transport, S2—hBN thickness dependence and baseline of $\boldsymbol{\Delta R(t)/R_0}$ curves, S3—Details of the two temperature model and reflectivity calculation, and S4—Evolution of the electronic and phonon temperature.

A.B. and B.J.L. were supported by the U.S. Army Research Laboratory and the U.S. Army Research Office under Contract/Grant No. W911NF-14-1-0653. D.G. and A.S. were supported by the National Science Foundation (NSF) under Contract No. PHY 1505556.

[1] Geim, A. K. and Grigorieva, I. V., "Van der Waals heterostructures," Nature **499**, 419–425 (2013).
[2] Dean, C. R., Young, A. F., Meric, I., Lee, C., Wang, L., Sorgenfrei, S., Watanabe, K., Taniguchi, T., Kim, P., Shepard, K. L. *et al.*, "Boron nitride substrates for high-quality graphene electronics," Nat. Nanotechnol. **5**, 722–726 (2010).
[3] Yankowitz, M., Xue, J., Cormode, D., Sanchez-Yamagishi, J. D., Watanabe, K., Taniguchi, T., Jarillo-Herrero, P., Jacquod, P., and LeRoy, B. J., "Emergence of superlattice dirac points in graphene on hexagonal boron nitride," Nat. Phys. **8**, 382–386 (2012).
[4] Xue, J., Sanchez-Yamagishi, J., Bulmash, D., Jacquod, P., Deshpande, A., Watanabe, K., Taniguchi, T., Jarillo-Herrero, P., and LeRoy, B. J., "Scanning tunnelling microscopy and spectroscopy of ultra-flat graphene on hexagonal boron nitride," Nat. Mater. **10**, 282–285 (2011).
[5] Wang, H., Strait, J. H., George, P. A., Shivaraman, S., Shields, V. B., Chandrashekhar, M., Hwang, J., Rana, F., Spencer, M. G., Ruiz-Vargas, C. S. *et al.*, "Ultrafast relaxation dynamics of hot optical phonons in graphene," Appl. Phys. Lett. **96**, 081917 (2010).
[6] Strait, J. H., Wang, H., Shivaraman, S., Shields, V., Spencer, M., and Rana, F., "Very slow cooling dynamics of photoexcited carriers in graphene observed by optical-pump terahertz-probe spectroscopy," Nano Lett. **11**, 4902–4906 (2011).
[7] Dawlaty, J. M., Shivaraman, S., Chandrashekhar, M., Rana, F., and Spencer, M. G., "Measurement of ultrafast carrier dynamics in epitaxial graphene," Appl. Phys. Lett. **92**, 42113–42116 (2008).
[8] Johannsen, J. C., Ulstrup, S., Cilento, F., Crepaldi, A., Zacchigna, M., Cacho, C., Turcu, I. C. E., Springate, E., Fromm, F., Raidel, C. *et al.*, "Direct view of hot carrier dynamics in graphene," Phys. Rev. Lett. **111**, 027403 (2013).
[9] Iglesias, J. M., Martín, M. J., Pascual, E., and Rengel, R., "Hot carrier and hot phonon coupling during ultrafast relaxation of photoexcited electrons in graphene," Appl. Phys. Lett. **108**, 043105 (2016).
[10] Lazzeri, M., Piscanec, S., Mauri, F., Ferrari, A. C., and Robertson, J., "Electron transport and hot phonons in carbon nanotubes," Phys. Rev. Lett. **95**, 236802 (2005).

[11] Pop, E., Mann, D., Cao, J., Wang, Q., Goodson, K., and Dai, H., "Negative differential conductance and hot phonons in suspended nanotube molecular wires," Phys. Rev. Lett. **95**, 155505 (2005).
[12] Lazzeri, M. and Mauri, F., "Coupled dynamics of electrons and phonons in metallic nanotubes: Current saturation from hot-phonon generation," Phys. Rev. B **73**, 165419 (2006).
[13] Gao, B., Hartland, G., Fang, T., Kelly, M., Jena, D., Xing, H., and Huang, L., "Studies of intrinsic hot phonon dynamics in suspended graphene by transient absorption microscopy," Nano Lett. **11**, 3184–3189 (2011).
[14] Bistritzer, R. and MacDonald, A. H., "Electronic cooling in graphene," Phys. Rev. Lett. **102**, 206410 (2009).
[15] Low, T., Perebeinos, V., Kim, R., Freitag, M., and Avouris, P., "Cooling of photoexcited carriers in graphene by internal and substrate phonons," Phys. Rev. B **86**, 045413 (2012).
[16] Hwang, E. H. and Das Sarma, S., "Surface polar optical phonon interaction induced many-body effects and hot-electron relaxation in graphene," Phys. Rev. B **87**, 115432 (2013).
[17] Ahn, S., Hwang, E. H., and Min, H., "Inelastic carrier lifetime in a coupled graphene/electron-phonon system: Role of plasmon-phonon coupling," Phys. Rev. B **90**, 245436 (2014).
[18] Bonini, N., Lazzeri, M., Marzari, N., and Mauri, F., "Phonon anharmonicities in graphite and graphene," Phys. Rev. Lett. **99**, 176802 (2007).
[19] Song, D., Wang, F., Dukovic, G., Zheng, M., Semke, E. D., Brus, L. E., and Heinz, T. F., "Direct measurement of the lifetime of optical phonons in single-walled carbon nanotubes," Phys. Rev. Lett. **100**, 225503 (2008).
[20] Yan, H., Song, D., Mak, K. F., Chatzakis, I., Maultzsch, J., and Heinz, T. F., "Time-resolved Raman spectroscopy of optical phonons in graphite: Phonon anharmonic coupling and anomalous stiffening," Phys. Rev. B **80**, 121403(R) (2009).
[21] Kang, K., Abdula, D., Cahill, D. G., and Shim, M., "Lifetimes of optical phonons in graphene and graphite by time-resolved incoherent anti-stokes Raman scattering," Phys. Rev. B **81**, 165405 (2010).
[22] Li, J., Miranda, H. P. C., Niquet, Y. M., Genovese, L., Duchemin, I., Wirtz, L., and Delerue, C., "Phonon-limited carrier mobility and resistivity from carbon nanotubes to graphene," Phys. Rev. B **92**, 075414 (2015).
[23] Gabor, N. M., Song, J. C. W., Ma, Q., Nair, N. L., Taychatanapat, T., Watanabe, K., Taniguchi, T., Levitov, L. S., Jarillo-Herrero, P., Sukhovatkin, V. *et al.*, "Hot carrier-assisted intrinsic photoresponse in graphene," Science **334**, 648–652 (2011).
[24] Duan, J., Wang, X., Lai, X., Li, G., Watanabe, K., Taniguchi, T., Zebarjadi, M., and Andrei, E. Y., "High thermoelectricpower factor in graphene/hBN devices," Proc. Natl. Acad. Sci. U. S. A. **113**, 14272–14276 (2016).
[25] Li, X., Magnuson, C. W., Venugopal, A., Tromp, R. M., Hannon, J. B., Vogel, E. M., Colombo, L., and Ruoff, R. S., "Large-area graphene single crystals grown by low-pressure chemical vapor deposition of methane on copper," J. Am. Chem. Soc. **133**, 2816–2819 (2011).
[26] Ahn, G., Kim, H. R., Ko, T. Y., Choi, K., Watanabe, K., Hong, B. H., Ryu, S., "Optical probing of electronic interaction between graphene and hexagonal boron nitride," ACS Nano **7**, 1533–1541 (2013).
[27] Das, A., Pisana, S., Chakraborty, B., Piscanec, S., Saha, S. K., Waghmare, U. V., Novoselov, K. S., Krishnamurthy, H. R., Geim, A. K., Ferrari, A. C. *et al.*, "Monitoring dopants by Raman scattering in an electrochemically top-gated graphene transistor," Nat. Nanotechnol. **3**, 210–215 (2008).
[28] Roberts, A., Cormode, D., Reynolds, C., Newhouse-Illige, T., Leroy, B. J., and Sandhu, A. S., "Response of graphene to femtosecond high-intensity laser irradiation," Appl. Phys. Lett. **99**, 051912 (2011).
[29] Lui, C. H., Mak, K. F., Shan, J., and Heinz, T. F., "Ultrafast photoluminescence from graphene," Phys. Rev. Lett. **105**, 127404 (2010).
[30] Jiang, L. and Tsai, H.-L., "Improved two-temperature model and its application in ultrashort laser heating of metal films," J. Heat Transfer **127**, 1167 (2005).
[31] Shah, J., *Ultrafast Spectroscopy of Semiconductors and Semiconductor Nanostructures* (Springer, 1996).
[32] Edgar, J. H., *Properties of Group III Nitrides* (Institution of Engineering and Technology, 1994).
[33] Chen, C. C., Li, Z., Shi, L., and Cronin, S. B., "Thermal interface conductance across a graphene/hexagonal boron nitride heterojunction," Appl. Phys. Lett. **104**, 081908 (2014).
[34] Li, X., Barry, E. A., Zavada, J. M., Buongiorno Nardelli, M., and Kim, K. W., "Surface polar phonon dominated electron transport in graphene," Appl. Phys. Lett. **97**, 232105 (2010).
[35] Mao, R., Kong, B. D., Kim, K. W., Jayasekera, T., Calzolari, A., and Buongiorno Nardelli, M., "Phonon engineering in nanostructures: Controlling interfacial thermal resistance in multilayer-graphene/dielectric heterojunctions," Appl. Phys. Lett. **101**, 113111 (2012).
[36] Pak, A. J. and Hwang, G. S., "Theoretical analysis of thermal transport in graphene supported on hexagonal boron nitride: The importance of strong adhesion due to π -bond polarization," Phys. Rev. Appl. **6**, 34015 (2016).
[37] Zhang, J., Hong, Y., and Yue, Y., "Thermal transport across graphene and single layer hexagonal boron nitride," J. Appl. Phys. **117**, 134307 (2015).
[38] Li, T., Tang, Z., Huang, Z., and Yu, J., "Interfacial thermal resistance of 2D and 1D carbon/hexagonal boron nitride van der Waals heterostructures," Carbon **105**, 566–571 (2016).
[39] Tielrooij, K. J. *et al.,* "Out-of-Plane Heat Transfer in van Der Waals Stacks : Electron-Hyperbolic Phonon Coupling," arXiv:1702.03766v1 [cond-mat.mes-hall] (2017).